Single Lanthanide-doped Oxide Nanoparticles as Donors in Fluorescence Resonance Energy Transfer Experiments

Didier Casanova,[†] Domitille Giaume,[‡] Thierry Gacoin,[‡] Jean-Pierre Boilot,[‡] and Antigoni Alexandrou*,[†]

Laboratory for Optics and Biosciences, CNRS UMR7645, INSERM U696, Ecole Polytechnique, F-91128 Palaiseau Cedex, France, and Laboratory of Condensed Matter Physics, CNRS UMR7643, Ecole Polytechnique, F-91128 Palaiseau Cedex, France

Received: May 25, 2006; In Final Form: July 27, 2006

We used lanthanide-ion doped oxide nanoparticles, $Y_{0.6}Eu_{0.4}VO_4$, as donors in fluorescent resonance energy transfer (FRET) experiments. The choice of these nanoparticles allows us to combine the advantages of the lanthanide-ion emission, in particular the long lifetime and the large Stokes shift between absorption and emission, with the detectability of the nanoparticles at the single-particle level. Using cyanine 5 (Cy5) organic molecules as acceptors, we demonstrated FRET down to the single-nanoparticle level. We showed that, due to the long donor lifetime, unambiguous and precise FRET measurements can be performed in solution even in the presence of large free acceptor concentrations. Highly efficient energy transfer was obtained for a large number of acceptor molecules per donor nanoparticle. We determined FRET efficiencies as a function of Cy5 concentration which are in good agreement with a multiple acceptor−multiple donor calculation. On the basis of the donor emission recovery due to acceptor photobleaching, we demonstrated energy transfer from single-nanoparticle donors in fluorescence microscopy experiments.

Introduction

Fluorescence resonance energy transfer (FRET) is a powerful tool for detecting biomolecule association and dissociation processes or conformational changes. It is based on the distance-dependent energy transfer between a donor and an acceptor via nonradiative dipole−dipole interaction and requires spectral overlap between the donor emission and the acceptor absorption.[1] This energy transfer results in a decrease of donor emission, an increase of acceptor emission, as well as a decrease of donor lifetime. The efficiency of the energy transfer can be measured by a quantification of these changes and used to determine the donor−acceptor distance.

FRET using organic fluorophores as donors and acceptors has been demonstrated down to the single-pair level[2] and is a broadly applied technique.[3] Recently, FRET experiments have been extended to nanoparticles used as donors, as in the case of quantum dots (QDs),[4] leading to nanosensor applications[5−8] or as multicolor emitters under single wavelength excitation in the case of silica nanoparticles containing different organic dyes.[9]

Several difficulties in FRET experiments arise due to the small Stokes shifts between absorption and emission of organic fluorophores and their broad emission spectra. To perform accurate distance measurements, it is important to discriminate against direct acceptor excitation and donor emission leaking into the acceptor emission channel. Solutions such as alternative excitation of donor and acceptor with two different excitation sources (ALEX-FRET) have been proposed to circumvent these problems.[10,11] These cross-talk problems can be minimized in systems with large Stokes shifts and narrow emission spectra. Along these lines, FRET (or LRET for luminescence resonance energy transfer) using lanthanide chelates[12−14] or, more recently, quantum dots[4−8] as donors has been demonstrated. In both these cases, the donor emission can be excited at wavelengths much shorter than the acceptor absorption thus minimizing direct acceptor excitation. Furthermore, the narrow donor emission, especially in the case of the atomic-like lanthanide emission,[14,15] does not overlap with the acceptor emission. In addition, quantum dots are photostable, in contrast to organic donors which are subject to fast photobleaching.

Lanthanide systems used as donors provide another crucial advantage: the excited-state lifetime is very long, in the millisecond range, because the electronic transitions involved, transitions among different f-electron configurations, are forbidden; they are in fact forced electric-dipole transitions due to mixing between $4f^n$ and $4f^{n-1}5d^1$ configurations induced by the noncentrosymmetric local crystalline field.[15,16] Thus, donor lifetime measurements are simple and precise. Furthermore, the FRET-induced acceptor emission shows the same decay behavior as the donor emission.[14] Therefore, it can be easily separated from any residual emission due to direct acceptor excitation whose decay will be in the nanosecond range. This FRET-induced long acceptor lifetime is an important FRET indicator because it is insensitive to incomplete pairing and allows measurements of small signals and consequently large distances. An additional advantage of lanthanide emission is its low anisotropy which leads to smaller errors in the determination of the orientation factor κ^2.[14,17]

Nevertheless, the emission of a chelate incorporating a single lanthanide ion is inherently weak (at the most one photon per lifetime period can be emitted) which renders the extrapolation of lanthanide-based FRET to the single donor case delicate. On the other hand, FRET involving a single QD donor has been

* To whom correspondence should be addressed. E-mail: antigoni.alexandrou@polytechnique.fr.
[†] Laboratory for Optics and Biosciences, Ecole Polytechnique.
[‡] Laboratory of Condensed Matter Physics, Ecole Polytechnique.

10.1021/jp063229v CCC: $33.50
Published on Web 09/02/2006

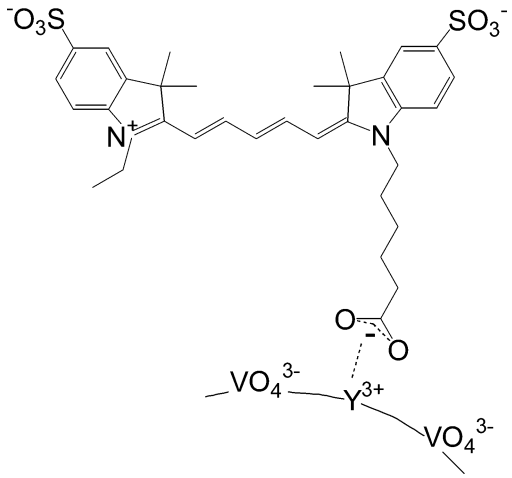

Figure 1. Schematic representation of a Cy5 molecule attached to the surface of a $Y_{0.6}Eu_{0.4}VO_4$ nanoparticle via complexation of its COO^- group to Y^{3+} (or Eu^{3+}) ions.

demonstrated,[6] but the QD blinking behavior[18] is a handicap for measurements at the single-particle level.

We here use lanthanide-doped oxide nanoparticles (NPs) as FRET donors to combine the assets related to lanthanide emission (long lifetime, large Stokes shift, narrow emission) with the capability of single-nanoparticle detection. Indeed, we have recently shown that these nanoparticles containing several thousands of lanthanide ions can be individually detected and functionalized for biomolecule labeling.[19] These nanoparticles are synthesized directly in water and show no emission intermittency owing to the large number of dopant ions in each nanoparticle. Due to the size of these nanoparticles (10−40 nm), several acceptor dyes can be attached to the nanoparticle surface thus increasing the FRET efficiency, similarly to what was shown for quantum-dot donors.[4]

$Y_{0.6}Eu_{0.4}VO_4$ nanoparticles were used as donors and Cy5 (Amersham) dye molecules as acceptors. We have exploited the fact that Cy5 molecules can be attached to the nanoparticles in a straightforward manner by complexation through their COO^- groups to Y^{3+} and Eu^{3+} ions at the surface of the nanoparticles (see Figure 1). Indeed, we have shown that citrate ligands form a complexing shell around the nanoparticles via their carboxylate groups leading to higher colloidal stability and smaller sizes.[20] In the following, we unambiguously demonstrate FRET in solution despite the presence of high concentrations of unbound Cy5 based on changes in donor intensity and lifetime as well as on the observation of a long-lived acceptor emission. The lifetime measurements are particularly facile due to the long lifetimes involved. The extracted FRET efficiencies as a function of acceptor concentration are in good agreement with a multiple donor−multiple acceptor model. Using a wide-field microscopy setup, we demonstrated FRET at the single-nanoparticle-donor level.

Experimental Methods

Nanoparticle Synthesis. $Y_{0.6}Eu_{0.4}VO_4$ nanoparticles were synthesized as in ref 21. A solution of $Y(NO_3)_3$ (48 mL, 0.1 M) and $Eu(NO_3)_3$ (32 mL, 0.1 M) is added dropwise to a solution of Na_3VO_4 freshly dissolved in water (80 mL, 0.1 M, pH 12.9) using a peristatic pump. The addition is stopped when the pH reaches the value of 9.1 (total addition of 60 mL). Counterions were eliminated by two centrifugations (11 400 g, 40 and 20 min) and dispersion of the precipitate in an ultrasound bath. A final purification by dialysis against pure water overnight

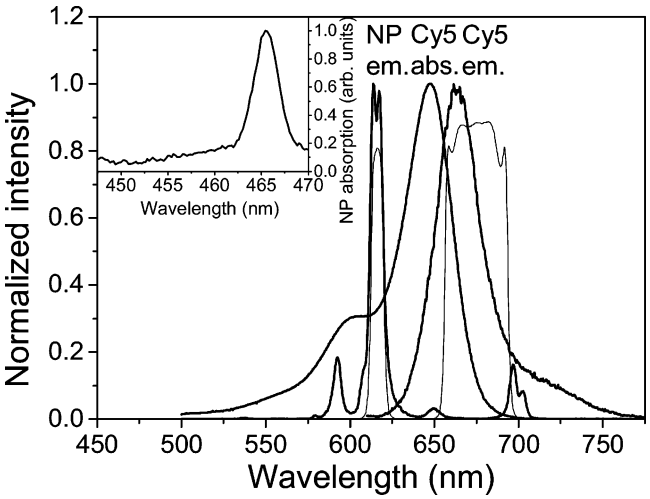

Figure 2. Emission spectrum of $Y_{0.6}Eu_{0.4}VO_4$ nanoparticles and absorption and emission spectrum of Cy5 (normalized data, thick lines) shown together with the transmission of the two filters used for the detection of the nanoparticle and Cy5 emission at 617 and 670 nm, respectively (thin lines). The inset shows the nanoparticle absorption spectrum in the range of interest here.

allows the complete elimination of the counterions (final conductivity, 86 $\mu S \cdot cm^{-1}$). These bare nanoparticles, in contrast to silica-coated ones, have a weak surface charge. Therefore, sonication in an ultrasound bath is applied before use to ensure complete dispersion of the nanoparticles.

We obtained nanoparticles with an average diameter of approximately 35 nm as determined by the luminosity histogram of individual nanoparticles.[22] Smaller nanoparticles with an average diameter of 17 nm were selected by retaining the supernatant after two centrifugations (11400 g, 10 min).[23] The average quantum yield q_D of the initial synthesis and of the smaller nanoparticles was equal to 0.18 and 0.07, respectively. The nanoparticle concentration is determined by dividing the concentration of vanadate (VO_4^{3-}) ions (obtained from absorption measurements at 280 nm) by the number of ions in the volume of a nanoparticle (4 vanadate ions per $(0.7\ nm)^3$).

Complexation with Cy5. We added 15 μL of a Cy5 solution of various concentrations in water to 200 μL of a nanoparticle solution with a fixed vanadate concentration in an ultrasound bath. NP-Cy5 experiments were conducted after a complexation reaction time of 45 min. We took no action to remove excess Cy5 molecules. Thus, a large fraction of the Cy5 molecules is in unbound form.

Fluorescence Measurements. The 465.8-nm Ar^+-ion laser line exciting the Eu^{3+} $^7F_{0,1}$−$^5D_2$ transition in the $Y_{0.6}Eu_{0.4}VO_4$ nanoparticles was used in most experiments.[19] For the determination of the direct acceptor excitation signal, the 457.9-nm Ar^+-ion line was used (no nanoparticle absorption in this case; see inset of Figure 2). The intensity at 457.9 nm was adjusted to correct for the difference in the Cy5 extinction coefficient, that is, to obtain the same Cy5 signal as under 465.8-nm excitation in the absence of nanoparticles.

Lifetime Measurements. The luminescence signal was detected at room temperature (20 °C) through a long-pass filter (OG5, Schott) for excitation laser rejection and either a 617/8M (Chroma) or a 670DF40 (Omega) filter (see Figure 2 for their transmission curves) using a photomultiplier (Hamamatsu, R636-10) and a digital oscilloscope (Tektronix, TDS3052). A reference signal from a vial containing water was subtracted. The laser was focused onto a mechanical chopper with an on-time of 0.63 ms, sufficient to reach steady-state excitation

conditions for the nanoparticles, and an off-time of 1.1 ms. For detection at 617 nm, a single chopper was used. For measurements at 670 nm, the large amount of unbound Cy5 emission can saturate the detector. Therefore, we used a second chopper, synchronized to the first one, placed in front of the detector, that opens 50 μs after switching off the laser excitation with the first chopper.

There is a small contribution of nanoparticle emission to the NP-Cy5 signal detected through the 670-nm filter due to the weak Eu^{3+} emission peak at 697 nm. The ratio between the intensities of a NP-only solution detected through the 617-nm and 670-nm filters was measured to be equal to 23.8. The NP-Cy5 signal shown in Figure 3B has therefore been corrected by subtracting the NP-Cy5 signal of Figure 3A divided by 23.8 (this correction is minor, on the order of 10%).

Microscopy Measurements. Images were recorded at room temperature (20 °C) on an inverted microscope under wide-field illumination, using an NA = 1.3 oil-immersion objective (Zeiss) and a liquid-nitrogen cooled CCD camera (Princeton Instruments LN/CCD-400-PB, 400 × 1340 pixels, back-illuminated). Fluorescence was selected using a dichroic mirror (530DCXR, Chroma). A second 5-mm thick dichroic mirror reflects light with wavelengths above 645 nm whereas the backside reflects wavelengths in the range 560−620 nm. Thus, two images shifted by 140 20-μm pixels are formed on the CCD. The 617- and 670-nm filters are used in front of the CCD to select light for the two images.

After a 45 min complexation time, the Cy5-coated nanoparticles were spin-coated on a silica coverslip. Rinsing of the coverslip with distilled water resulted in the removal of the free Cy5 molecules.

Calculation of the FRET Efficiency

The efficiency of energy transfer, E, is defined as the probability for the excited donor to return to its ground state by energy transfer to the acceptor

$$E = \frac{k_T}{k_T + k_D} \tag{1}$$

where k_T is the rate of energy transfer to the acceptor and k_D is the total rate of all other radiative and nonradiative donor decay processes.

The FRET efficiency can be expressed in terms of R_0, the distance at which $E = 0.5$

$$E = \frac{1}{1 + \left(\frac{R}{R_0}\right)^6} \tag{2}$$

R_0 is a function of the spectral overlap between donor emission and acceptor absorption, the donor and acceptor relative orientation, the donor quantum yield, and the index of refraction.[14]

Taking into account multiple acceptors at distances R_i with associated energy transfer rates k_{T_i}, eq 1 becomes

$$E = \frac{\sum_i k_{T_i}}{\sum_i k_{T_i} + k_D} \tag{3}$$

leading to

$$E = \frac{1}{1 + \frac{1}{\left(\sum_i \frac{R_0}{R_i}\right)^6}} \tag{4}$$

In our case, the above calculation has to be performed for every lanthanide (Eu^{3+} in our case) ion inside the nanoparticle. Thus, we are in a multiple donor−multiple acceptor configuration.

Since energy transfer induces a loss of donor emission intensity, the FRET efficiency can also be written as

$$E = 1 - \frac{I_{D_A}}{I_D} \tag{5}$$

where I_{D_A} (I_D) is the donor emission intensity in the presence (absence) of the acceptor. In a lanthanide-doped nanoparticle, the donor intensity corresponds to the sum of the individual lanthanide-ion emissions, $I_{D_{Aj}}$ and I_{D_j}, in the presence and the absence of the acceptor, respectively

$$E = 1 - \frac{\sum_j I_{D_{Aj}}}{\sum_j I_{D_j}} = 1 - \frac{I_{D_j}\sum_j (1 - E_j)}{N_{Eu} I_{D_j}} = \frac{\sum_j E_j}{N_{Eu}} \tag{6}$$

where N_{Eu} is the number of Eu^{3+} ions in a nanoparticle and E_j is the FRET efficiency associated with an individual lanthanide ion. Thus, the FRET efficiency for a nanoparticle corresponds to the average of all FRET efficiencies of individual lanthanide ions.

Replacing rates by lifetimes in eq 1, we obtain

$$E = 1 - \frac{\tau_{D_A}}{\tau_D} = 1 - \frac{\tau_{A_D}}{\tau_D} \tag{7}$$

where τ_D (τ_{D_A}) and τ_{A_D} are the excited-state lifetimes of the donor in the absence (presence) of the acceptor and the acceptor lifetime due to FRET excitation by the donor, respectively. The second part of eq 7 is justified as follows: in the case of a long-lived donor excited state and a short-lived organic-molecule acceptor excited state, energy transfer will take place as long as the donor remains at the excited state. Once the excitation is transferred to the acceptor, it will decay with the short acceptor characteristic time. The limiting parameter in this case is the FRET-induced appearance of excited acceptor molecules which is governed by the donor excited-state decay. Therefore, the FRET-induced acceptor emission will follow the donor decay. This long-lived acceptor emission will thus have a lifetime τ_{A_D} equal to τ_{D_A}. In contrast, the emission due to direct acceptor excitation will decay in nanoseconds.

The FRET efficiency can also be calculated from the FRET-induced acceptor emission intensity I_{A_D}

$$E = \frac{I_{A_D}/q_A}{I_{A_D}/q_A + I_{D_A}/q_D} \tag{8}$$

This equation translates the fact that the FRET efficiency is the ratio of donor excitations transferred to the acceptor to the total number of donor excitations. The emitted intensity I_{A_D} (I_{D_A}) can be converted into excited-state population density by dividing by the acceptor (donor) quantum yield, q_A (q_D).

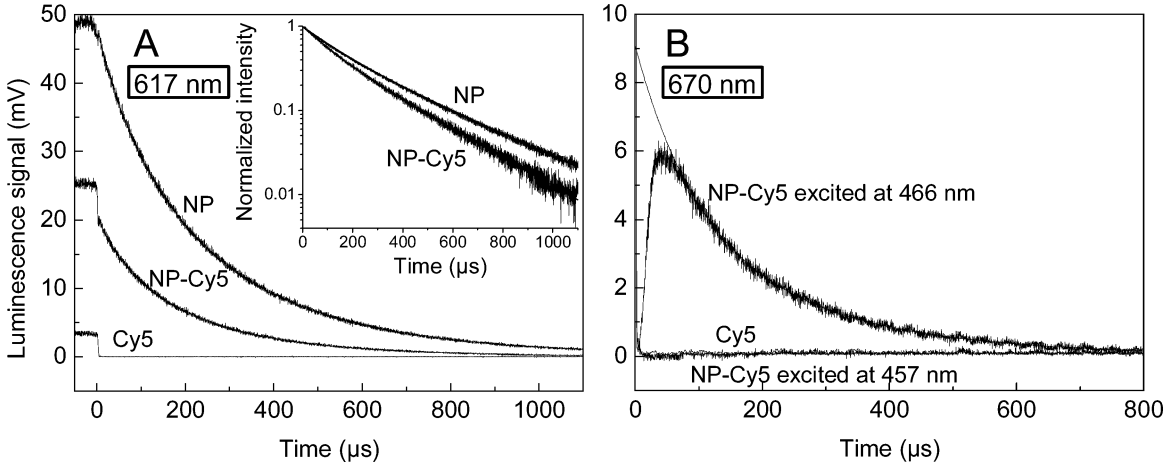

Figure 3. Decay curves measured using the 617-nm filter (A) and the 670-nm filter (B). The concentration of the 35-nm $Y_{0.6}Eu_{0.4}VO_4$ nanoparticles and Cy5 was 17 nM (4.4 mM in vanadate ions) and 70 μM, respectively. The 0 of the time scale corresponds to switching off the laser excitation. (A) $Y_{0.6}Eu_{0.4}VO_4$ nanoparticles in the absence and in the presence of Cy5 as well as Cy5 alone. The inset shows the normalized decay curves of $Y_{0.6}Eu_{0.4}VO_4$ nanoparticles in the absence and in the presence of Cy5 together with biexponential fits (due to the excellent agreement with the experiment, the fits are not distinguishable). (B) Cy5 emission in the presence and in the absence of $Y_{0.6}Eu_{0.4}VO_4$ nanoparticles after excitation at 466 nm and Cy5 emission in the presence of $Y_{0.6}Eu_{0.4}VO_4$ nanoparticles after excitation at 458 nm. A biexponential was used to fit the FRET-induced Cy5 decay after 70 μs and is extrapolated to time 0. The detection chopper opens at 50 μs.

Experimentally, detected intensities, I^{det}, are available which can be converted into emitted intensities by dividing with the detection efficiency at the donor and acceptor emission wavelength, η_D and η_A, respectively

$$E = \frac{1/q_A}{\frac{1}{q_A} + \frac{I^{det}_{D_A}}{I^{det}_{A_D}} \frac{\eta_A}{\eta_D} \frac{1}{q_D}} \tag{9}$$

Results and Discussion

Figure 2 shows the absorption and emission spectra of Cy5 and Eu-doped nanoparticles. We calculated the normalized spectral overlap between donor emission and acceptor absorption, J,[14] by taking into account only the $^5D_0-^7F_2$ and $^5D_0-^7F_4$ forced electric-dipole transitions centered at 617 and at 697 nm, respectively. The $^5D_0-^7F_1$ and $^5D_0-^7F_3$ transitions centered at 593 and 650 nm, respectively, are magnetic dipole transitions[16,24] and do not contribute to FRET. Using the average index of refraction of YVO_4 $n = 2.0704$ at 617 nm, an orientation parameter $\kappa^2 = {}^2/_3$ assuming random orientation of the donor and acceptor transition dipoles, and the quantum efficiency of the nanoparticles $q_D = 0.18$ (0.07 for the smaller nanoparticles), we obtained $R_0 = 41.9$ Å (35.8 Å for the smaller nanoparticles).

Ensemble FRET Measurements. We used the narrow 466-nm Eu^{3+} absorption line to excite the 35-nm nanoparticles and recorded the fluorescence decay of a NP, a NP−Cy5, and a Cy5 solution at the donor (Figure 3A) and at the acceptor emission wavelength (Figure 3B) using two different filters centered at 617 and 670 nm, respectively (see Figure 2). In the presence of Cy5, both the nanoparticle emission intensity and decay time are reduced indicating the presence of energy transfer to Cy5 (see Figure 3A). In addition, a small abrupt decrease (faster than our time resolution) is observed right after the laser excitation is switched off. This abrupt decrease is due to a small fraction of the Cy5 emission centered at 663 nm leaking through the 617-nm filter (see Figure 2). The Cy5-only control solution shows the same abrupt drop and thus confirms this interpretation. We can calculate the FRET efficiency using eq 5: $E = 1 - 19.9/48.5 = 0.59$ where I_{D_A} was taken equal to the intensity after the initial fast drop.

The NP-only emission after 40 μs can be fitted to the equation: $y = 42\% \exp(-t/130\ \mu s) + 58\% \exp(-t/331\ \mu s)$. The two different lifetimes can be explained as follows: the energy of the $^5D_0-^7F_6$ Eu^{3+} transition nearly corresponds to the third harmonic of the OH vibrational mode in water molecules. This is a well-known nonradiative decay processes for Eu^{3+} ions and has been demonstrated in our colloidal nanoparticles.[24] Obviously, the Eu^{3+} ions close to the surface of the nanoparticle will be more affected by this nonradiative channel thus leading to shorter excited-state lifetimes. The NP emission in the presence of Cy5 after 40 μs can be fitted to the following: $y = 40\% \exp(-t/100\ \mu s) + 60\% \exp(-t/260\ \mu s)$. Both the short and the long lifetime of the NP emission are reduced in the presence of Cy5. Using eq 7 and the average lifetimes[25] in the presence and absence of Cy5, we can calculate the FRET efficiency: $E = 1 - 159/201 = 0.21$.

The apparent discrepancy between the FRET efficiency calculated using the emission intensities and the lifetimes is explained as follows: the Eu ions close to the surface of the nanoparticles can be located at very small distances from a Cy5 molecule. For these ions, the FRET efficiency will be practically 1, the intensity emitted by them will be negligible, and the lifetimes of the small remaining fraction of emitted intensity will be extremely short. The decay curve of the nanoparticle emission will therefore show little trace of this contribution and will be dominated by the Eu ions closer to the center of the nanoparticles where individual-ion FRET efficiencies E_j are lower. The ratio of the nanoparticle emission intensity in the presence and the absence of acceptor (eq 5), on the other hand, takes into account contributions from ions both at the surface and in the volume of the nanoparticles and gives a more accurate determination of the FRET efficiency. This interpretation is confirmed by the simulations discussed below.

Let us now turn to the emission of Cy5 at 670 nm (Figure 3B). In the absence of FRET, the decay time of the Cy5 emission is in the nanosecond range. In contrast, the Cy5 emission due to energy transfer from the nanoparticles will follow the decay time of the NP emission and will thus be in the millisecond range. This is indeed what is observed in Figure 3B (NP-Cy5 curve) and is irrefutable evidence that FRET takes place. The temporal discrimination of FRET-induced Cy5 emission is a

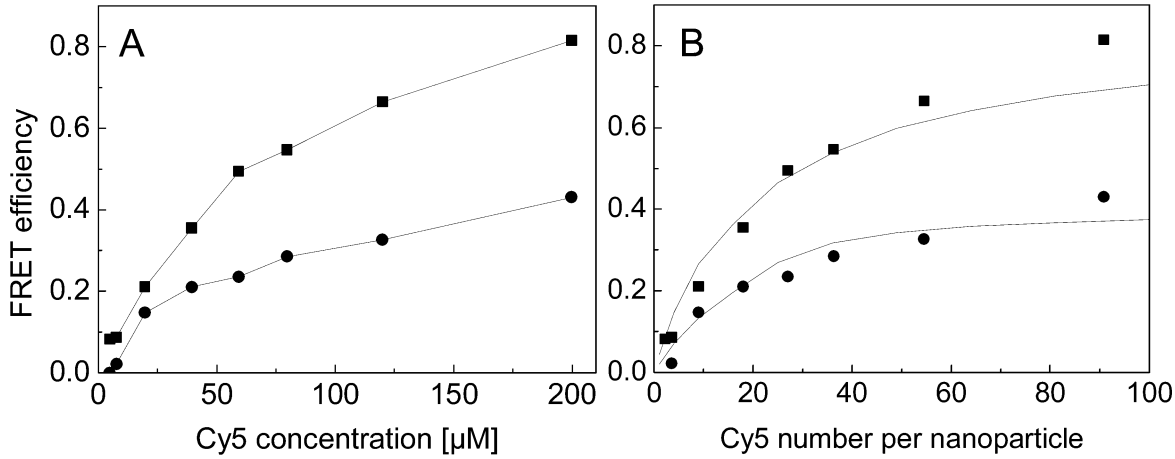

Figure 4. (A) Experimental data: FRET efficiency as a function of Cy5 concentration estimated from the nanoparticle emission intensity in the presence and absence of Cy5 (eq 5, squares) or from the nanoparticle emission lifetime in the presence and absence of Cy5 (eq 7, circles). The 17-nm nanoparticle concentration was 0.12 μM (3.6 mM in vanadate ions). The second approach underestimates the FRET efficiency. The lines are a guide to the eye. (B) Theoretical FRET efficiency as a function of the number of Cy5 molecules per nanoparticle calculated using the nanoparticle emission intensity or the nanoparticle emission lifetime (solid lines). The experimental data of (A) are superimposed (see text).

powerful tool because it allows measurements free from direct acceptor excitation signal (which is short-lived) and independent of acceptor-only concentrations. As a further control, we recorded the fluorescence of a Cy5-only solution as well as the signal of a NP-Cy5 solution excited at 458 nm where there is no nanoparticle absorption (see inset of Figure 2) and thus no FRET. In both these cases, no long-lived signal was observed.

The decay time of the FRET-induced Cy5 emission for times longer than 70 μs was fitted with the biexponential: $y = 58\% \exp(-t/96\ \mu s) + 42\% \exp(-t/252\ \mu s)$. As discussed above, the FRET efficiency calculated from the average acceptor lifetime,[25] $\tau_{A_D} = 130\ \mu$s, using eq 7 is underestimated because the short lifetime contributions due to Eu^{3+} ions close to the nanoparticle surface are cut off by the rejection of the first 50 μs by the second chopper in front of the detector. For the same reasons, the FRET efficiency calculated using eq 9 is underestimated. Indeed, by extrapolating to time 0 the fit to the decay curve for times longer than 70 μs, we find $I_{A_D} = 9.1$ and $E = 0.17$, where we have used $q_D = 0.18$ and $q_A = 0.28$ and $\eta_A/\eta_D = 1.42$.

Comparison wih Simulations. We then repeated the above experiments as a function of the total Cy5 concentration using nanoparticles with an average diameter of 17 nm.[23] The FRET efficiencies obtained using the donor intensities and lifetimes are shown in Figure 4A. We again find that the determination based on the donor lifetimes underestimates the FRET efficiency. Quite high transfer efficiencies ($E > 0.8$) are observed for large Cy5 concentrations.

To compare our experiments to simulations, we considered ellipsoidal nanoparticles with a homogeneous distribution of Eu ions and a homogeneous distribution of a varying number of Cy5 molecules on their surface.[26] We then calculated for each Eu ion, j, its distance to the different Cy5 molecules, R_i, the associated FRET efficiency, E_j, using eq 4 and subsequent emission intensity, $I_{D_{Aj}}$, and lifetime, $\tau_{D_{Aj}}$, using eqs 5 and 7, respectively, where τ_D was taken to be equal to the average experimental lifetime (208.4 μs). The individual decay curves were then summed to give the nanoparticle decay curve whose value at $t = 0$ gives I_{D_A}. The NP lifetime curves consist of a fast decaying part due to Eu ions close to the surface followed by a slower decay due to Eu ions in the volume of the nanoparticle. To better approach the experimental conditions, the decay curves were fitted to biexponentials between 40 and 1100 μs, the average lifetime giving τ_{D_A}. The FRET efficiencies obtained from these theoretical I_{D_A} and τ_{D_A} values are shown in Figure 4B. As expected, the FRET efficiency determined from the donor lifetime is underestimated.

TABLE 1: FRET Efficiency, *E*, Obtained from the Nanoparticle Emission Intensity Change and Nanoparticle Average Lifetime Values, $\langle\tau_{DA}\rangle$[25]

total Cy5/NP concentration ratio	bound Cy5 molecules per NP	NP size (nm)	$\langle\tau_{D_A}\rangle$ (μs)	*E*
4118		35	159	0.59
1665	91	17	119	0.81
1000	55	17	140	0.66
665	36	17	149	0.55
495	27	17	159	0.49
330	18	17	165	0.35
165	9	17	178	0.21
65	4	17	204	0.09
42	2	17	208	0.08

[a] The error bar is approximately 10%. The lifetime of the 35 (17) nm nanoparticles in the absence of acceptors was 201 (208.4) μs. The numbers of bound Cy5 molecules per nanoparticle were determined from the comparison between the experimental data and the simulations (see Figure 4).

The *x*-axis in Figure 4A (Cy5 concentration) can be translated into the number of Cy5 molecules per nanoparticle by dividing with the NP concentration (0.12 μM). The ratio of total to bound Cy5 molecules is determined by the complexation reaction equilibrium constant K

$$K = \frac{[Y^{3+} - Cy5]}{[Y^{3+}][Cy5]} \tag{10}$$

where $[Y^{3+}]$ stands for the total Y^{3+} and Eu^{3+} concentration. Very good agreement between the experimental and theoretical data can be obtained by assuming a ratio of total to bound Cy5 molecules equal to 18.3 (see Figure 4B). The FRET efficiencies and lifetime values obtained for the various Cy5/nanoparticle ratios are recapitulated in Table 1. On the basis of the total Y^{3+} and Eu^{3+} concentration at the surface of the 17-nm nanoparticles (estimated to be equal to 445 μM), this ratio implies $K = 130\ M^{-1}$. This value should be considered as an estimate of the order of magnitude due to uncertainties in nanoparticle size and concentration and due to the fact that the Y^{3+} and Eu^{3+} ions interacting with Cy5 molecules are concentrated on the nanoparticle surfaces and do not diffuse independently.

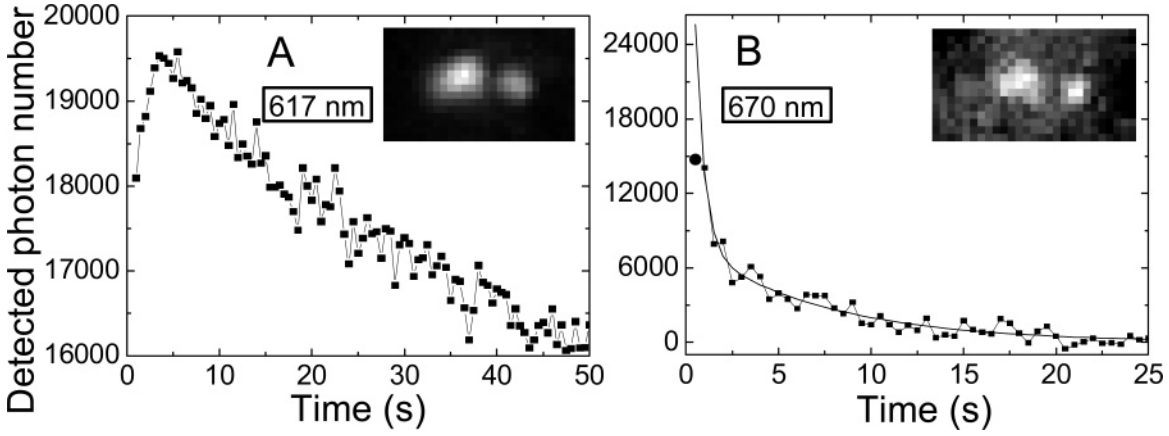

Figure 5. Detected photons per image through (A) the 617-nm filter and (B) the 670-nm filter as a function of prior illumination time for a single Cy5-coated nanoparticle spin-coated on a silica coverslip observed using wide-field dual-color fluorescence microscopy (squares and solid lines as a guide to the eye; excitation wavelength, 466 nm; intensity at the sample, 2 kW/cm^2; integration time, 500 ms). The concentration of the 35-nm nanoparticles and Cy5 used in the complexation reaction was 4.2 nM (1.1 mM in vanadate ions) and 18 μM, respectively. In (B), the solid line is a biexponential fit to the Cy5 emission decay; the circle corresponds to a first image taken under 458-nm excitation. The insets are images showing Cy5-coated nanoparticles and correspond to the first 466-nm illumination. The Cy5-coated nanoparticle on the right was used to obtain the detected photon numbers shown here.

Single-donor FRET Experiments. We also demonstrated energy transfer on the single-donor level. For this purpose, we used an inverted microscope setup to observe 35-nm nanoparticles deposited by spin-coating on a silica coverslip after complexation with Cy5. We have previously shown that these lanthanide-doped nanoparticles are observable on the single-particle level[19] after spin-coating on a coverslip at suitable dilution levels. The detection of single nanoparticles is confirmed by a comparison between the measured and calculated number of detected photons per second.[19,22] In the present case, we performed dual-color imaging (through the 617- and the 670-nm filter) to simultaneously image light emitted by the nanoparticles and by Cy5. We first checked, by imaging a nanoparticle-only coverslip, that the bright spots due to single nanoparticles in the 617-nm image (see ref 19) gave rise to no signal in the 670-nm image. Similarly, the Cy5 emission leak in the 617-nm image was negligible.

In the case of Cy5-coated nanoparticles, emission in both the 617- and the 670-nm image was observed (see insets of Figure 5). To determine which part of the Cy5 emission at 670 nm is due to direct excitation, we recorded a single image under 458-nm excitation (no excitation of the nanoparticles and thus no FRET) followed by a series of images under 466-nm excitation. Figures 5A and B show the number of photons detected for the bright spot on the right in the insets at 617 and 670 nm, respectively, as a function of prior illumination time. The Cy5 signal (Figure 5B) photobleaches almost completely within 5 s. The nanoparticle signal (Figure 5A), on the contrary, shows an increase concomitant with the Cy5 photobleaching. This increase is then followed by a slow decrease which is the behavior normally observed for single nanoparticles in the absence of Cy5 (see Figure 1F of ref 19). Note that only the usual slow decrease of the nanoparticle emission was observed for nanoparticles without Cy5 (showing no signal in the 670-nm image). The nanoparticle emission increase concomitant with the Cy5 emission decrease is clear evidence of energy transfer taking place between the single nanoparticle and Cy5 molecules at its surface. As the Cy5 molecules photobleach, the energy loss channel due to FRET disappears and the nanoparticle emission increases.

To determine the FRET efficiency, we subtracted the Cy5 signal measured under 458-nm excitation (direct acceptor excitation) from the Cy5 signal under 466-nm excitation (direct excitation + FRET signal) to obtain I_{A_D}. The Cy5 signal under 466-nm excitation was determined by fitting the decay curve as a function of illumination time to a biexponential and by extrapolating to the value corresponding to the first illumination sequence. I_{D_A} was taken equal to the value corresponding to the first image under 466-nm excitation. Using eq 9, we obtained $E = 0.24$ for the nanoparticle on the right in the inset of Figure 5 and $E = 0.17$ (standard deviation, 0.07) as an average over 13 nanoparticles. This FRET efficiency is weaker than that expected from ensemble measurements for the same relative nanoparticle and Cy5 concentrations ($E = 0.59$). There are two explanations for this difference: (i) Part of the Cy5 molecules at the surface of the nanoparticles are removed during the rinsing of the coverslip (see Experimental Methods section) since the complexation is a reversible process. (ii) The I_{D_A} value is slightly overestimated because it corresponds to the second (instead of the first) illumination sequence and some Cy5 photobleaching has already taken place.

Conclusions

We have shown that lanthanide-doped nanoparticles are very promising as donors in FRET experiments. Indeed, the long lifetime, the large Stokes shift, and the narrow emission of these nanoparticles render FRET experiments particularly straightforward and feasible even in the presence of large amounts of unbound acceptor. The nanosecond acceptor emission due to direct acceptor excitation can be easily distinguished from the much longer-lived sub-millisecond FRET-induced acceptor fluorescence. A large number of acceptor (Cy5) molecules can be bound to the nanoparticles, and for large Cy5 concentrations, FRET efficiencies larger than 0.8 have been obtained. A comparison with simulations demonstrates that, in this multiple donor−multiple acceptor configuration with a whole range of donor−acceptor distances, the most reliable estimation of FRET efficiency is the one based on the donor intensity in the presence and absence of acceptor. The combination of the advantages of lanthanide-ion luminescence and the presence of a large number of lanthanide ions in nanometer-sized particles allowed the observation of energy transfer from a single nanoparticle donor.

We expect energy transfer to a single acceptor per nanoparticle to be detectable for smaller nanoparticles (5−10 nm) in ensemble measurements. Currently, $Y_{0.6}Eu_{0.4}VO_4$ nanoparticles

excited through a Eu^{3+} absorption line are individually detectable for sizes down to 15 nm.[22] To achieve single-pair energy transfer, excitation of the nanoparticles in the UV exploiting the much higher absorption coefficient of the oxide matrix should be used.

Ensemble FRET measurements using these nanoparticles as donors can be used to measure protein−protein, protein−DNA, or oligonucleotide interaction processes. We have recently functionalized these lanthanide-doped nanoparticles with amine groups. They can then be attached to the amine group of a biomolecule using a homobifunctional cross-linker (formation of peptide bonds between the nanoparticle and the linker and between the linker and the biomolecule).[27] Thus, binding of a protein to lanthanide nanoparticles should allow us to determine its interaction network with other proteins labeled with the acceptor fluorophore. Furthermore, nanoparticles conjugated to specific recognition molecules such as receptors, can be quenched by using acceptor-labeled ligand analogues and used as nanosensors detecting the replacement of the analogue by the ligand via the disappearance of FRET, similarly to what was proposed for FRET-based TNT QD sensors.[5] For very small analyte amounts, as in the case of signaling molecules liberated by cells, the capability of detection on the single-donor level may be essential. More generally, all types of FRET applications could profit from the features of these nanoparticle donors: straightforward lifetime measurements, experiments exempt from necessity of free acceptor removal as well as from donor photobleaching and blinking problems.

Acknowledgment. We thank Manuel Joffre for a useful discussion and the DGA (Délégation Générale pour l'Armement) and the Fonds National pour la Science (AC Dynamique et Réactivité des Assemblages Biologiques) for financial support.

References and Notes

(1) Förster, T. In *Modern Quantum Chemistry*; Sinanoglou, O., Ed.; Academic: New York, 1965; p 93.

(2) Ha, T.; Enderle, T.; Ogletree, D. F.; Chemla, D. S.; Selvin, P. R.; Weiss, S. *Proc. Natl. Acad. Sci. U.S.A.* **1996**, *93*, 6264.

(3) Lakowicz, J. R. *Principles of Fluorescence Spectroscopy*; Kluwer Academic: New York, 1999.

(4) Clapp, A. R.; Medintz, I. L.; Mauro, J. M.; Fisher, B. R.; Bawendi, M. G.; Mattoussi, H. *J. Am. Chem. Soc.* **2004**, *126*, 301.

(5) Goldman, E. R.; Medintz, I. L.; Whitley, J. L.; Hayhurst, A.; Clapp, A. R.; Uyeda, H. T.; Deschamps, J. R.; Lassman, M. E.; Mattoussi, H. *J. Am. Chem. Soc.* **2005**, *127*, 6744.

(6) Zhang, C.-Y.; Yeh, H.-C.; Kuroki, M. T.; Wang, T.-H. *Nat. Mater.* **2005**, *4*, 826.

(7) Chang, E.; Miller, J. S.; Sun, J. T.; Yu, W. W.; Colvin, V. L.; Drezek, R.; West, J. L. *Biochem. Biophys. Res. Commun.* **2005**, *334*, 1317.

(8) Medintz, I. L.; Clapp, A. R.; Brunel, F. M.; Tiefenbrunn, T.; Uyeda, T.; Chang, E. L.; Deschamps, J. R.; Dawson, P. E.; Mattousi, H. *Nat. Mater.* **2006**, *5*, 581.

(9) Wang, L.; Tan, W. *Nano Lett.* **2006**, *6*, 84.

(10) Kapanidis, A.; Lee, N. K.; Laurence, T. A.; Doose, S.; Margeat, E.; Weiss, S. *Proc. Natl. Acad. Sci. U.S.A.* **2004**, *101*, 8936.

(11) Lee, N. K.; Kapanidis, A.; Wang, Y.; Michalet, X.; Mukhopadhyay, J.; Ebright, R. H.; Weiss, S. *Biophys. J.* **2005**, *88*, 2939.

(12) Selvin, P. R.; Rana, T. M.; Hearst, J. E. *J. Am. Chem. Soc.* **1994**, *116*, 6029.

(13) Selvin, P. R.; Hearst, J. E. *Proc. Natl. Acad. Sci. U.S.A.* **1994**, *91*, 10024.

(14) Selvin, P. R. *Annu. Rev. Biophys. Biomol. Struct.* **2002**, *31*, 275.

(15) Blasse, G.; Grabmeier, B. C. *Luminescent Materials*; Springer-Verlag: Berlin, 1994.

(16) Carnall, W. T.; Goodman, G. L.; Rajnak, K.; Rana, R. S. *J. Chem. Phys.* **1989**, *90*, 3443.

(17) Reifenberger, J. G.; Snyder, G. E.; Baym, G.; Selvin, P. R. *J. Phys. Chem. B* **2003**, *107*, 12862.

(18) Brokmann, X.; Hermier, J.-P.; Desbiolles, P.; Bouchaud, J.-P.; Dahan, M. *Phys. Rev. Lett.* **2003**, *90*, 120601.

(19) Beaurepaire, E.; Buissette, V.; Sauviat, M.-P.; Giaume, D.; Lahlil, K.; Mercuri, A.; Casanova, D.; Huignard, A.; Martin, J.-L.; Gacoin, T.; Boilot, J.-P.; Alexandrou, A. *Nano Lett.* **2004**, *4*, 2079.

(20) Huignard, A.; Buissette, V.; Laurent, G.; Gacoin, T.; Boilot, J.-P. *Chem. Mater.* **2002**, *14*, 2264.

(21) Huignard, A.; Gacoin, T.; Boilot, J.-P. *Chem. Mater.* **2000**, *12*, 1090.

(22) Casanova, D.; Giaume, D.; Beaurepaire, E.; Gacoin, T.; Boilot, J.-P.; Alexandrou, A. Unpublished results.

(23) The mean size of the nanoparticles was obtained from TEM images which show ellipsoids with mean values for 603 nanoparticles of the long (short) axis equal to 22.2 (12.7) nm and standard deviations equal to 10.7 and 5.6 nm, respectively. The diameter of a circle of equal surface is 16.7 nm.

(24) Huignard, A.; Buissette, V.; Franville, A.-C.; Gacoin, T.; Boilot, J.-P. *J. Phys. Chem. B* **2003**, *107*, 6754.

(25) The inverse average lifetime is taken equal to the weighted mean of the inverse times used for the biexponential fit.

(26) The axis lengths of the ellipsoids were taken equal to the mean values determined from the TEM images, 22.2 and 12.7 nm. The third axis length was taken equal to the mean value determined from the other two (16.7 nm).

(27) Casanova, D.; Giaume, D.; Martin, J.-L.; Gacoin, T.; Boilot, J.-P.; Alexandrou, A. Unpublished results.